

Article

Need for Standardization: Influence of Artificial Canal Size on Cyclic Fatigue Tests of Endodontic Instruments

Sebastian Bürklein ^{1,*}, Paul Maßmann ², David Donnermeyer ², Karsten Tegtmeier ² and Edgar Schäfer ¹

¹ Central Interdisciplinary Ambulance in the School of Dentistry, Albert-Schweitzer-Campus 1, Westphalian Wilhelms-University, Building W 30, 48149 Münster, Germany; eschaef@uni-muenster.de

² Department of Periodontology and Operative Dentistry, Albert-Schweitzer-Campus 1, Westphalian Wilhelms-University, Building W 30, 48149 Münster, Germany; p_mass02@uni-muenster.de (P.M.); David.Donnermeyer@ukmuenster.de (D.D.); Karsten.Tegtmeier@ukmuenster.de (K.T.)

* Correspondence: sebastian.buerklein@ukmuenster.de; Tel.: +49-251-8347051; Fax: +49-251-8347894

Abstract: The aim was to evaluate the influence of artificial canal size on the results of cyclic fatigue tests for endodontic instruments. Dynamic cyclic fatigue at body temperature using continuous tapered nickel–titanium F6-SkyTaper instruments (Komet, Lemgo, Germany), size 25/.06 with an amplitude of 3 mm, was tested in four different simulated root canals: (A) size of the instrument +0.02 mm (within the tolerances of the instruments); (B) +0.05 mm; (C) +0.10 mm; (D) parallel tube with 1.25 mm in diameter. The artificial canals (angle of curvature 60°, radius 5.0 mm, center of curvature 5.0 mm) were produced by a LASER-melting technique. Time and cycles to fracture, and lengths of the fractured instruments were recorded and statistically analyzed (Student–Newman–Keuls; Kruskal–Wallis test). Time to fracture significantly increased with increasing size of the artificial canals in the following order: A < B, C < D ($p < 0.05$). Length of separated instruments continuously decreased with increasing canal sizes. The parallel tube produced the significantly shortest fragments ($p < 0.05$). Within the limitations of this study, dynamic cyclic fatigue of endodontic instruments depends on the congruency of the instruments' dimensions with that of the artificial canals. In future cyclic fatigue testing, due to the closer match of canal and instrument parameters, it is necessary to adjust the artificial canal sizes to the size of the instruments within the manufacturing tolerances of the instruments.

Keywords: artificial canal; congruence; body temperature; dynamic fatigue tests; fracture resistance; ISO; nickel–titanium instruments



Citation: Bürklein, S.; Maßmann, P.; Donnermeyer, D.; Tegtmeier, K.; Schäfer, E. Need for Standardization: Influence of Artificial Canal Size on Cyclic Fatigue Tests of Endodontic Instruments. *Appl. Sci.* **2021**, *11*, 4950. <https://doi.org/10.3390/app11114950>

Academic Editor: Seok Woo Chang

Received: 12 May 2021

Accepted: 26 May 2021

Published: 27 May 2021

Publisher's Note: MDPI stays neutral with regard to jurisdictional claims in published maps and institutional affiliations.



Copyright: © 2021 by the authors. Licensee MDPI, Basel, Switzerland. This article is an open access article distributed under the terms and conditions of the Creative Commons Attribution (CC BY) license (<https://creativecommons.org/licenses/by/4.0/>).

1. Introduction

Endodontic instruments have undergone multiple changes in design and metallurgy in the last decades. With specific heat treatment procedures, manufacturers have produced increasingly flexible alloys and claimed to reduce the incidence of instrument fracture during root canal preparation [1]. Fracture of nickel–titanium (NiTi) endodontic instruments as an iatrogenic complication during root canal treatment or retreatment is undesired by both patients and clinicians, as it may negatively influence endodontic treatment outcome by preventing a proper chemo-mechanical disinfection of the entire root canal system, i.e., inaccessible areas beyond the obstruction [2]. The incidence of NiTi file separation is highly variable (0.14–5%) and depends on numerous factors such as study design, number and kind of teeth included, clinician's experience, instrument type, single- or multi-use of instruments, and metallurgy [3–5]. Whereas clinicians can influence the longevity of instruments as a function of the rotational speed [6–8], the kind of motion [9], the pre-flaring procedures [10], glide path preparation [11], the number of uses [12], and sterilization cycles [13], patient-related factors such as root canal anatomy with its inherent angle and radius of the curvature [7,14] are immutable. Instrument parameters are also decisive,

whereby a bigger instrument diameter leads to a shorter lifetime span in cyclic fatigue tests [15]. Additionally, the core mass is decisive for stress generation and fracture susceptibility [16]. However, the most recent studies showed a markedly reduced incidence when using modern endodontic NiTi instruments [5,17,18].

Instruments may fracture due to cyclic fatigue, torsional stress, or a combination of both [19]. Cyclic fatigue is caused by the continuous changes in compression and tension at the inner and outer curvatures depending on the rotational speed, the angle, and the radius of the curvature [20]. Torsional fracture occurs when the tip region of the instrument is locked by engaging into the dentinal walls and the coronal portion, and when the shaft continues rotating [21]. The properties (i.e., fracture resistance, flexibility) of the instruments are becoming more and more important as the number of instruments used for the entire enlargement of the root canals is minimized when using modern systems with a reduced sequence of instruments or even single-file systems. Thus, the number of cycles and the level of stress onto the instruments are significantly increased. Cyclic fatigue may represent a clinically relevant parameter that can provide evidence about the lifetime of instruments in the root canal, by testing a single parameter under standardized laboratory conditions [22].

However, cyclic fatigue testing is not included in the ISO standard for endodontic instruments. The ISO 3630:1 specification (current version 2019-08) addresses only resistance to fracture by twisting and angular deflection in chapter 7.4, and it recommends standard atmosphere conditions at 23 °C (± 2 °C) [23].

Numerous setups and devices for cyclic fatigue testing have been proposed and implemented. This fully explains the finding of a recent review elucidating that results in different studies investigating identical instruments differed by up to more than 300% [24]. Hence, results were not comparable. Actually, there is no consensus among scientists concerning crucial parameters such as the angle and radius of curvature and the location of the center of the curvature, despite the influence of these parameters being scientifically proven [25]. The same applies to the vertical amplitude during testing. Although, in 1986, Dederich and Zakariasen already presented a dynamic testing device that allowed investigating the cyclic fatigue resistance of endodontic rotary instruments by implementing a vertical amplitude (pure axial motion) [26], in the past, most tests were performed statically [24]. Static tests offer a major limitation because instruments are loaded at only one specific section. Dynamic testing definitively overcomes this limitation by simulating the dynamic in-and-out movements (pecking motion, brushing, stroking) of an endodontic treatment, representing a more clinically relevant setup. The trend is toward an amplitude of 3 mm with a frequency of about 0.5 Hz. Ideally, all procedures should be performed at body temperature [27], because the temperature during testing significantly influences the time to fracture of the instruments due to the specific metallurgy and different A_f temperatures of the alloys [28–31].

Nevertheless, no further details concerning the congruency of the simulated artificial root canals and the diameter of the instruments have been proposed. There is a consensus that instruments should rotate freely without having friction to the artificial canals walls in order to prevent additional torsional load. However, a looser fit leads to less constant trajectories of load during testing [32].

Since Plotino et al. expressed a need for standardization for cyclic fatigue testing of NiTi rotary instruments to ensure uniformity of methodology and to allow comparable results more than 10 years ago, nothing noteworthy has happened [20]. An exception is the latest presentation of a new test machine allowing a real-time measurement of bending force of the instruments when performing cyclic fatigue tests [33]. Only few efforts have been made to create more standardized artificial canals [34,35], and many authors did not specify the diameters. The influence of the congruency between the instrument and the testing tube/artificial canal is still unclear.

Thus, the aim of the study was to investigate the influence of different artificial root canal sizes on the fracture resistance of NiTi instruments when performing cyclic fatigue

tests. The null hypothesis (H0) tested was that the size and the corresponding congruence of the matching artificial canals have no impact on the fracture resistance of the tested instruments.

2. Materials and Methods

2.1. Sample Size Calculation

The sample size calculation was based on the means and standard deviations of five instruments tested under identical conditions as described in the main study. Analysis revealed an effect size of >1.0 . A markedly lower effect size of 0.4 served for calculation. Using the parameters of an alpha (α) level of 0.05 (5%) and a (β) beta level of 0.20 (20%) (i.e., power = 80% at a 5% significance level) and a large effect size of 0.4 revealed a sample size of 19 in each group. Thus, 20 instruments in each group were used (total = 80).

2.2. Manufacturing of the Artificial Canals

Following a technical drawing (Figure 1), an artificial root canal size 25/.06 (+0.02 mm) was created using Geomagic Freeform software (3D Systems, McLean, VA, USA). Additional canals with the same conicity but an increased diameter (+0.05 mm, +0.10 mm) and a parallel tube (diameter 1.25 mm) were also designed [34,35].

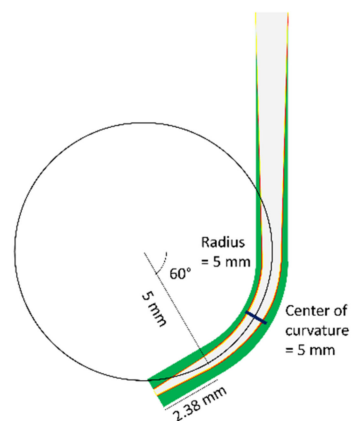


Figure 1. Technical drawing of the artificial root canals with the illustration of superimposed artificial root canals; gray = instrument size +0.02 mm, yellow = +0.05 mm, red = +1.0 mm, green = parallel tube 1.25 mm.

Canals were exactly 16 mm long, corresponding to the working part of the instruments, and they terminated in a circle at their end in order to have an open system allowing a replacement and a kind of reservoir of the lubricant used.

STL data of artificial canals were transferred into a CoCr model using a digital metal laser sintering (DMLS) method (Infinident Solutions, Darmstadt, Germany). During this special manufacturing process, a cobalt-based metal ceramic alloy was applied evenly in the form of fine-grain powder with the assistance of a so-called recoater on a building panel and then melted layer by layer using a 200 W Yb (ytterbium) fiber laser with shielding gas (nitrogen (N₂)). After the melting process of a layer, the platform panel was lowered according to a predefined layer thickness (20–40 μ m), and the subsequent layer was prepared accordingly until the whole object was finished. Afterward, unique cleaning and thermal post-processing procedures were necessary for stress-relief annealing. Finally, the objects were sandblasted.

2.3. Cyclic Fatigue Testing

During the cyclic fatigue test, the instruments rotated freely in the artificial stainless-steel canal with 60° curvature and a 5 mm radius, with the center of curvature at 5 mm from the apex (Figures 1 and 2). The inner diameter of the canal was designed to accommodate

the size and taper of the tested instrument (Figure 3). In order to prevent the instruments from slipping out of the tube, the artificial canals were covered with tempered glass [36]. Glycerin oil warmed to body temperature served as a lubricant and was continuously refreshed during testing to prevent any friction. All instruments were tested at 300 rpm and 2.2 N/cm torque following the manufacturer's recommendations. A continuous axial oscillating movement was generated by a rotating drive disc with an eccentric mount 1.5 mm from the central axis (total amplitude = 3 mm) with a frequency of 1 cycle/2 s (Hertz) and served for the simulation of the dynamic up-and-down movements (picking motion, stroking) during root canal treatment (Figure 4). To achieve a correct positioning of the handpiece, it was fixed in a 3D printed and assembled handpiece holder, especially fabricated for the present study (Figures 4 and 5). The test machine allowed a free adjustment of the different components to each other.

An incubator served for maintenance of body temperature to guarantee a constant temperature (37 ± 1 °C) throughout the entire procedure. Additionally, the temperature inside the artificial canal was checked permanently using thermo-K couples with a frequency of 50 Hz (Figure 4).

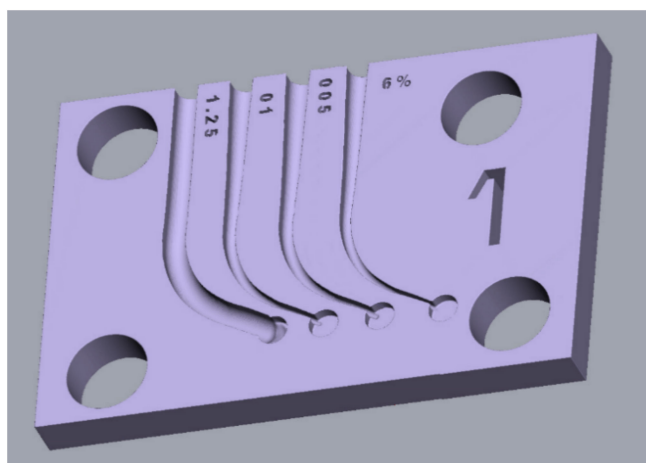


Figure 2. Artificial root canals designed with Geomagic Freeform software.

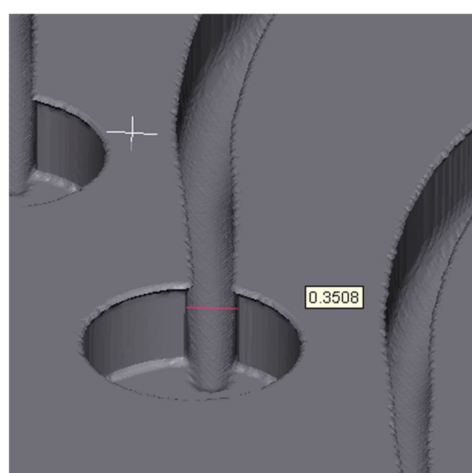


Figure 3. Close-up from of the artificial root canal (size +0.10 mm) with the diameter of the apical constriction in millimeters.

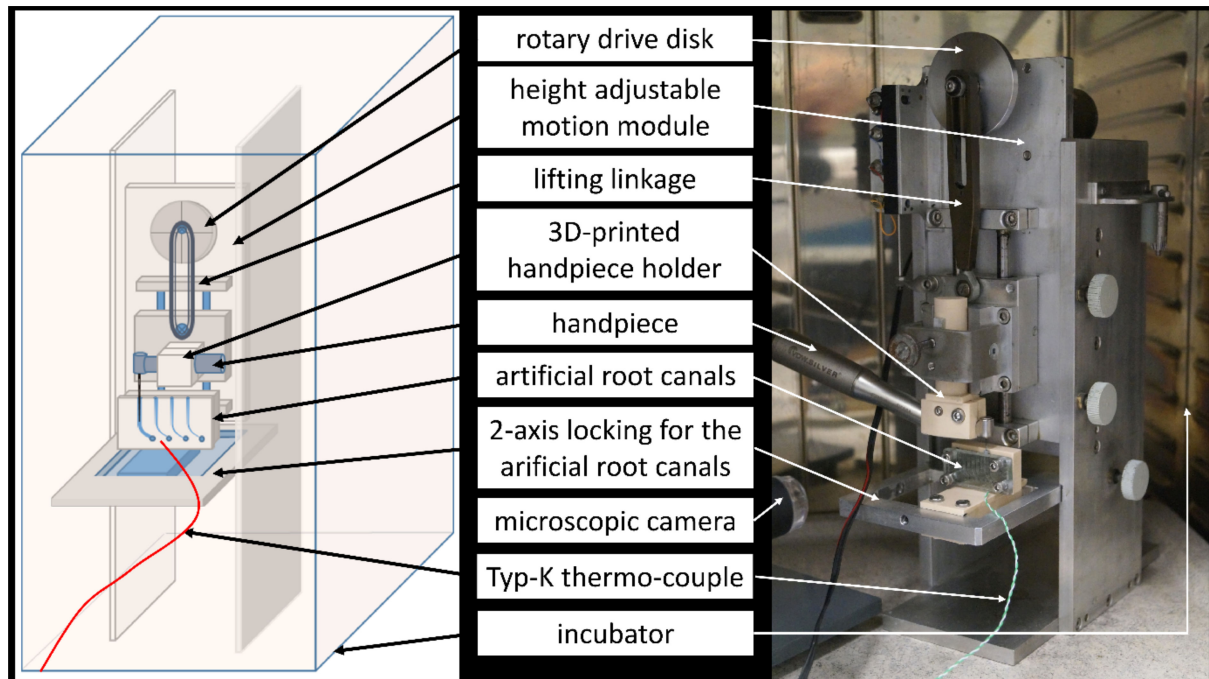


Figure 4. Schematic drawing and original photograph of the dynamic cyclic fatigue testing device placed in an incubator.

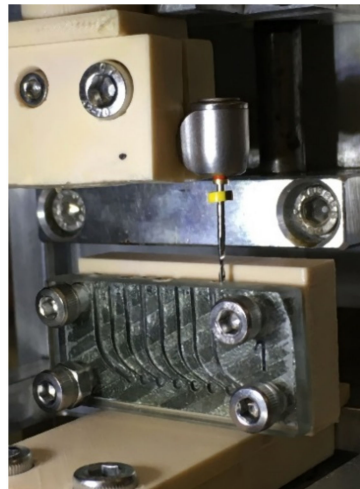


Figure 5. Detailed view of the setup: artificial root canals covered with tempered glass with an inserted instrument.

The time recording started when setting the instrument into rotation and inserting it into the artificial root canal. The fracture was observed visually through a microscopic camera (Figure 4), and the time to fracture was recorded. The NCF (number of cycles to failure) was evaluated as follows:

$$\text{NCF} = \frac{\text{time to fracture [s]}}{60} \times \text{speed [rpm, rotations per minute]}. \quad (1)$$

The lengths of the fractured segments were measured using a digital caliper (Mitutoyo 500–196–30 Absolute AOS Digimatic; Mitutoyo Corporation, Kawasaki, Japan).

2.4. Fractographic Analysis

The surfaces were screened for characteristic fractographic appearance of a fatigued metallic material using a laser scanning microscope (Keyence VK-X1000, Keyence Cor-

poration, Osaka, Japan). In the cross-section, the typical fatigue fracture pattern consists of crack initiation, propagation, and catastrophic fracture with dimples. Dimples on the entire fracture surface are characteristic for cyclic fatigue fractures, whilst torsional failures show circular abrasion marks and dimples near the center of rotation on the fracture surface [19,37,38].

2.5. Statistical Analysis

The normality of the data distribution and the homogeneity of variances were tested using Kolmogorov–Smirnov and Levene tests. The time to fracture and the number of cycles to failure were normally distributed and analyzed using ANOVA and the post hoc Student–Newman–Keuls test. The length of the fractured fragments showed a nonparametric distribution. Thus, data were statistically analyzed by Kruskal–Wallis test. The statistical analysis was performed using SPSS 20 software (SPSS Inc., Chicago, IL, USA). The level of significance was set at $p < 0.05$.

3. Results

The time and cycles to fracture and the fracture length of instruments with standard deviation, minimum, and maximum values are listed in Table 1.

The fracture resistance of the instruments depended on the diameter of the artificial canals. The time and cycles to fracture in the matching canal (+0.02 mm) were significantly shorter compared to all other canals, and the parallel tube created the significantly longest lifetime of instruments ($p < 0.05$). The 0.05 mm and 0.10 mm tubes did not differ concerning all investigated parameters ($p > 0.05$).

The length of the fractured fragments was significantly shorter in the parallel tube ($p < 0.05$), whereas all other groups did not differ significantly ($p > 0.05$).

Table 1. Time and cycles to fracture and fracture length of instruments with standard deviation, minimum, and maximum values ($p < 0.05$). Values sharing the same superscript letters are not statistically different at a 0.05-level.

Tube	Time to Fracture (s)	SD	Min	Max	Cycles to Fracture	SD	Min	Max	Fracture Length (mm)	SD	Min	Max
Original	277.0 ^a	25.97	228	336	1846.8 ^a	173.14	1520	2240	2.91 ^a	0.88	2.36	4.12
+0.02 mm	302.2 ^b	36.86	244	361	2016.8 ^b	245.70	1626	2406	2.75 ^a	0.47	1.74	3.52
+0.10 mm	304.6 ^b	42.29	230	381	2030.7 ^b	281.91	1533	2540	2.72 ^a	0.38	2.22	3.74
+1.2 mm	393.5 ^c	42.12	293	472	2622.3 ^c	280.78	1953	3147	2.09 ^b	0.32	1.58	3.11
<i>p</i> -value		<0.05				<0.05				<0.05		

All fracture surfaces showed typical signs of cyclic fatigue (Figure 6). Areas of fatigue propagation were easily detectable by the shiny lines/areas and the large ripped portions.

The steady crack growth region presented different sizes (outlined with a dotted line) and origins (yellow arrows) (Figure 6B–D). Stress propagation was visible due to the striations (white arrows) (Figure 6A). Lastly, the cyclic stress reduced instruments core mass and led to catastrophic failure, represented by the rippled areas.

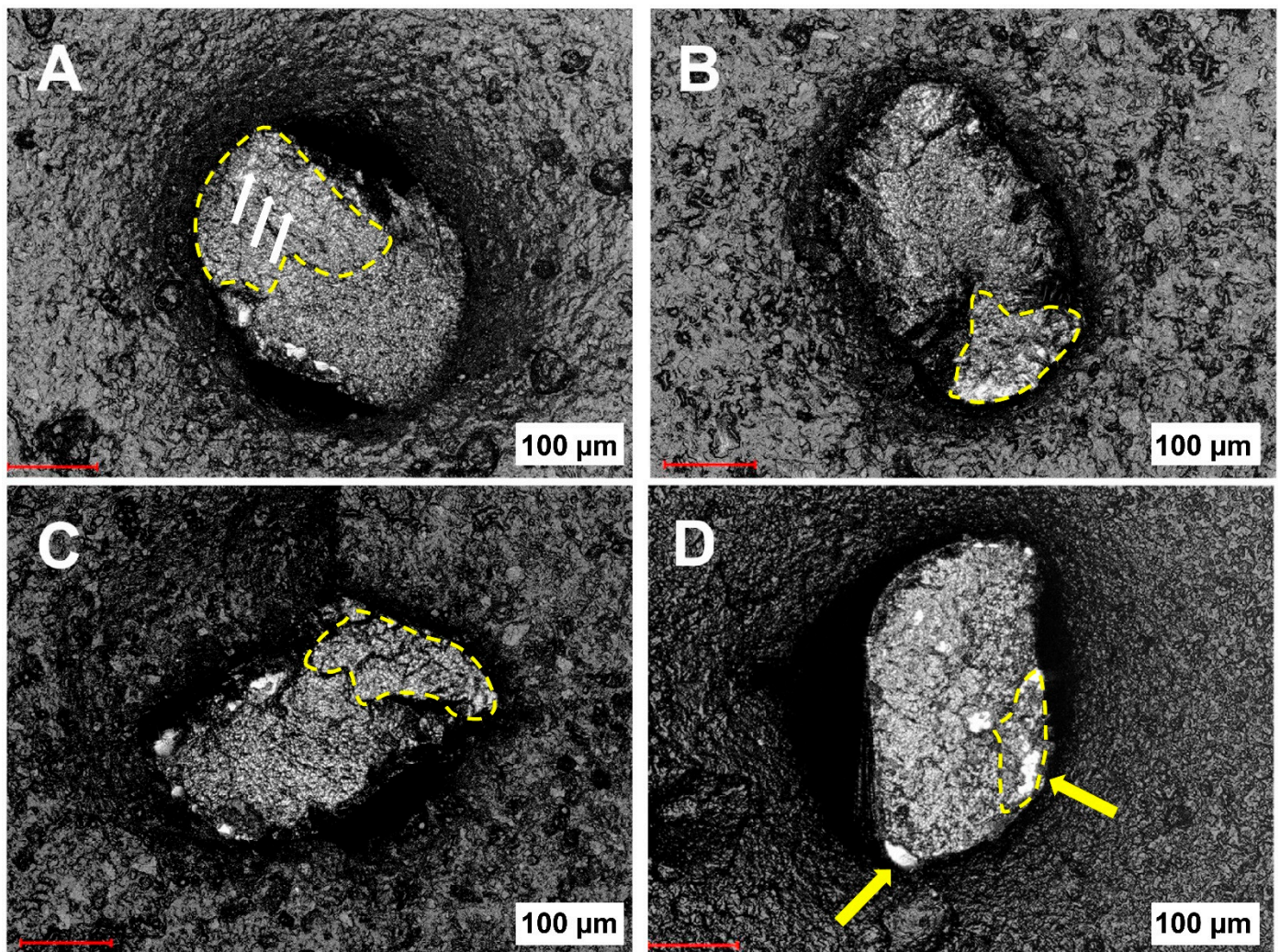


Figure 6. Exemplary surfaces of fractured instruments: (A) matching canal (+0.02 mm). The fractured cross-section the instrument shows an area of fatigue propagation = striation area (white arrows), delimited by the shiny dotted line, visible starting from the origin of the fracture at the top of the file. A huge rippled area nearly over the complete cross-section is visible. (B) +0.05 mm. (C) +0.10 mm. Typical for instruments with S-shaped cross-section, fractures usually start in the regions with the largest distance to the neutral fiber (propagation area = yellow dotted line). (D) Parallel tube (1.25 mm). The fractured cross-section shows two propagation areas (yellow dotted line and arrows)—one starting from the cutting edge at the bottom, and the other at the right side in the convex and straight portion.

4. Discussion

Due to the results obtained in the present study, the null hypothesis (H0) was rejected, as the size and congruency of the artificial canals exerted a significant effect on the cyclic fatigue resistance of endodontic rotary instruments.

4.1. Material and Curvature Parameter of the Artificial Root Canals

Canals were produced by a LASER melting approach using a computer aided design program. This technique allows machining highly complex constructions with a material density of almost 100% that can be produced in an automated process, which cannot be manufactured with conventional processes such as casting or milling or only with enormous effort. The dimensional accuracy of the artificial canals was checked with a laser scanning microscope to guarantee the correct dimensions.

Various methods for measurement of root canal curvature are available and have been proposed since Schneider introduced his method exclusively assessing the angle of

curvatures [39]. Pruett et al. were the first to describe a method of root canal curvature measurement and explained how to make curved stainless-steel guide tubes (CST) for testing the cyclic fatigue resistance of endodontic instruments [40]. Schäfer et al. implemented the radius of curvature as an additional parameter for a more distinct definition of root canal curvatures [41]. Overall, the parameters in the present study were based on those most often used in comparable previous studies [22]. The center of curvature served as an additional aspect specifying the location of the curvature in addition to the radius. Thus, the parameters were set at 60° curvature, radius 5 mm, and center of curvature at 5 mm from the “apex” based on Pruett’s method with slight modifications. When transferring the current setup, the defined angle of curvature of 60° would result in an angle of about 40° according to Schneider’s method.

In general, different setups were proposed for cyclic fatigue testing. Angles varied between 45° and 90°, and the radius and the center of curvature showed a wide range between 2 and 6 mm. Due to the lack of standardization and the absence of any ISO standard for cyclic fatigue testing, the currently available studies are hardly comparable [22].

4.2. Temperature and Amplitude

Temperature has been shown to exert a major impact on the results of cyclic fatigue testing. The modern endodontic instruments are flexible and ductile due to proprietary heat treatment procedures [1]. During active canal preparation, instruments were used inside the oral cavity and, thus, the surrounding/working temperature changed from room temperature to a temperature close to body temperature. De Hemptinne et al. [34] reported that the mean intracanal temperature during root canal preparation is about 35.1 °C (± 1 °C) [42].

The crystal lattice of NiTi depends on the A_f temperature. Whereas conventional super elastic (SE) NiTi instruments are in the austenitic phase at or below body temperature and exhibit superelastic properties [1], heat-treated alloys such as M-Wire, R-Phase, CM-wire, Gold, and Blue-Wire present higher A_f temperatures and are essentially in the martensite/R phase state in the working environment at body temperature. This enhancement offers promising results, concerning the cyclic resistance, but the impact on torsional failure is inconclusive [22]. However, conditions during testing should be as realistic as possible and experiments were, therefore, performed at body temperature.

Water-based glycerin at 37 °C—constantly refreshed—served as a lubricant in order to reduce friction of the instruments to the walls of the artificial canals and to avoid additional development of heat. Common alternatives for this purpose represent air cooling or using synthetic oil [22], but a water-based lubricant seemed to be closer to clinical practice and was established in cyclic fatigue tests [24].

Root canal preparation is always a dynamic process. Manufacturers demand keeping the instruments in motion and not static. Depending on the instrument used and the manufacturer’s instructions, the amplitude varies. Picking motions from 1 to 3 mm or even larger strokes from 5 or more mm may be suited for proper mechanical preparation. As a compromise, a 3 mm axial oscillating motion served for the simulation of dynamic preparation in the present study.

4.3. Congruency/Fitting of the Artificial Root Canals to Instruments

In nearly all studies reported in the endodontic literature concerning cyclic fatigue, instruments were set into rotation/reciprocation in glass or metal tubes, grooved blocks, or metal blocks. Only a minority of the studies mentioned fitting of the instrument in the artificial canal or tube; hence, congruency remains unclear. As Plotino et al. highlighted, the so-called “free space” between the canal wall and the instrument, also termed the shape of the artificial tube, is crucial for the load of the endodontic instruments, because trajectories differ due to different shapes [43]. It can be assumed that the impact of the radius of curvature on the obtained results may have been overestimated in many studies. This may represent a reason for the huge variability in the results of identical instruments

tested under different experimental conditions [22]. A lower fit results in a lower curvature of the endodontic file and a lower load onto the instrument (Figure 7).

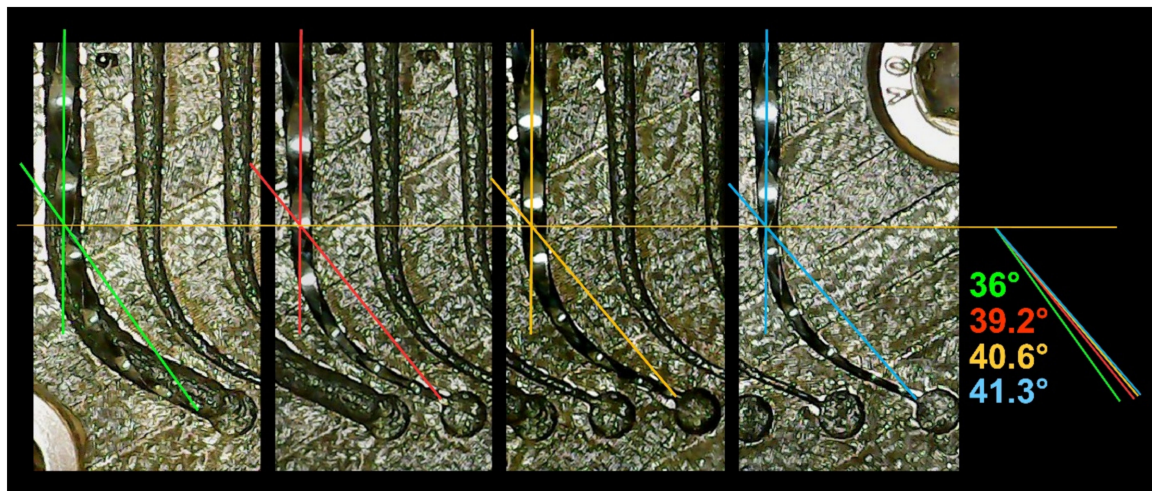


Figure 7. Straightening of the instrument due to increasing diameter of the artificial root canal. From left to right: parallel tube with a diameter of 1.25 mm (green), instrument size +0.10 mm (red), instrument size +0.05 mm (orange), matching tube = instrument size +0.02 mm (blue).

The manufacturing tolerance of endodontic instruments allowed by the ISO standard is ± 0.02 mm [23]. Therefore, the dimension in the narrowest canal was set within these tolerances at 0.02 mm bigger than the instrument size. The subsequent diameters of the artificial canals were larger at +0.05 mm and +0.10 mm. A parallel tube with a diameter of 1.25 mm served as a control.

The present results clearly demonstrated a significant difference between the narrowest size of the artificial canal (instrument size +0.02 mm) and the +0.05 mm and +0.10 mm canal sizes. (Table 1). The cyclic fatigue resistance of instruments was significantly reduced in the matching artificial canal (same conicity as the instrumented tested; diameter +0.02 mm), whereas the length of the fractured fragments did not differ compared to the subsequent artificial canal sizes. No significant differences occurred between the 0.05 mm and 0.10 mm groups with respect to any of the evaluated parameters ($p > 0.05$). Only the parallel tube showed significant differences regarding all values examined ($p < 0.05$). This raises the question whether the sizes of the artificial canals should be set at the manufacturing tolerance level as preset in the ISO specification (i.e., ± 0.02 mm) or even up to 0.10 mm larger. However, the instrument tolerances were valid in both directions, i.e., larger and thinner compared to the given sizes. This may allow a kind of range in matching congruency (Table 2). Differences between the instrument sizes and the tube were smallest in the matching tube and did not exceed a factor of 1.17. Whereas, in the +0.05 mm and +0.10 mm groups, the factors were between 1.10–1.30 and 1.30–1.52, respectively, the parallel tube offered a 4.40- to 5.20-fold increase in diameter.

Nevertheless, when looking at the standard deviations of time and cycles to fracture (Table 1), only in the matching size group did these values not exceed the 10% level of the mean values; therefore, the deviations were relatively the smallest and the results seem to be the most reliable.

Table 2. Percentage increase in diameter between instrument tip and artificial canal sizes in relation to different instruments according to manufacturing tolerances.

Percentage Increase in Diameter between Instrument Tip and Artificial Canal Sizes in Relation to Manufacturing Tolerances				
Instrument (Size # 25)	Matching Tube Instrument Size +0.02 # 27/100 mm	Instrument Size +0.05 mm # 35/100 mm	Instrument Size +0.10 mm # 45/100 mm	Parallel Tube 1.2 mm # 120/100 mm
Lower tolerance # 23	+17%	+30%	+52%	+522%
Exact size # 25	+8%	+20%	+40%	+480%
Upper tolerance # 27	+0%	+11%	+30%	+444%
Instrument (Size # 15)	Matching Tube Instrument Size +0.02 # 17/100 mm	Instrument Size +0.05 mm # 25/100 mm	Instrument Size +0.10 mm # 35/100 mm	Parallel Tube 1.2 mm # 120/100 mm
Lower tolerance # 13	+31%	+92%	+269%	+923%
Exact size # 15	+15%	+67%	+233%	+800%
Upper tolerance # 17	+0%	+47%	+206%	+706%

Nevertheless, a major limitation of the present study is the fact that only instruments with a size # 25 were investigated. It is important to consider that the relative increase in the diameters decreases with increasing instrument size (Table 2); for example, an instrument with a size # 15 would have ranges of 0–31%, 17–54%, 47–95%, and 706–923% in the different artificial canals representing identical artificial canal sizes adapted to the instrument. Thus, the importance of congruence and minimum free space between the artificial canal and the endodontic instrument seems desirable to achieve a better guidance of the instruments during testing. Additionally, the angle of curvature decreases when testing instruments in larger canals. When determining true curvatures in the present study using Schneider’s method, the angles were 41.2°, 40.6°, 39.2°, and 36.0°, respectively (Figure 7). The decreasing length of the fractured fragments with increasing diameter of the artificial canals provides further evidence of the changing stress trajectories that result in maximum stress closer to the center of curvature.

Using matching artificial canals did not cause any torsional load (Figure 6). Fractographic examination of the fractured surfaces revealed failure due to cyclic fatigue. Fracture schemes were in accordance with those reported in previous studies [44,45]. Fatigue failure is characterized by macroscopical ‘brittleness’. Whereas, in lateral views, some minor plastic deformation may be visible on both sides of the fractures [19], the cross-sectional views usually show a crack propagation perpendicular to the direction of maximum stress, successively reducing the intact mass of the cross-section (Figure 6A–D). Finally, the fracture results in catastrophic failure due to a ‘final’ load cycle that induces a fast and unstable growth of the crack [37]. Hence, the cross-sectional analysis is crucial to determine the fracture mode (fatigue, torsional, or mixed mode) [19,38].

Nonetheless, fracture of NiTi endodontic instruments under clinical conditions appears to be mainly caused by a single overload event (causing ductile fracture) rather than solely by alloy fatigue due to the multiple loading cycles [46]. Overload may be attributed to many factors (i.e., iatrogenic factors) caused by the active preparation of the root canal. Hence, the longevity of endodontic instruments is highly variable, as the instruments are subjected to multiple dynamic forces due to the cutting/shaping action and axial load in the presence of intracanal debris combined with engagement into the dentinal walls during root canal treatment. Therefore, despite the knowledge of fatigue resistance of NiTi instruments from cyclic fatigue testing [22], direct extrapolation of laboratory parameters to the clinical situation should be done with caution.

However, all these considerations suggest that, in further studies, it is reasonable to test instruments with other sizes, tapers, and metallurgies in artificial canals with a diameter in the range of the instrument. This unique setup may help overcoming the controversial discussions about cyclic fatigue testing of endodontic instruments by guaranteeing well-

standardized and reproducible experimental conditions, regardless of whether rotating or reciprocating instruments are tested. Despite the anatomical and morphological diversity of root canals, the best possible standardization should be mandatory, at least in laboratory studies, to allow comparisons regarding the fracture resistance of endodontic instruments.

5. Conclusions

Cyclic fatigue testing depends on artificial root canal diameter. Better-standardized experimental setups guarantee results that are more reliable.

Proposed parameters are as follows:

- matching diameter of artificial canals = instrument size plus tolerances (0.02 mm);
- angle of curvature 60°;
- radius 5 mm;
- center of curvature at 5 mm from the tip;
- dynamic testing with an amplitude of 3 mm;
- frequency of amplitude about 0.5 Hz;
- body temperature (37 °C);
- glycerin as a lubricant.

Further studies with different instruments, instrument sizes, and kinematics are required to support the suggested settings in cyclic fatigue tests of endodontic instruments.

Author Contributions: Conceptualization, S.B. and E.S.; methodology, S.B. and D.D.; software, K.T.; formal analysis, S.B. and E.S.; investigation, S.B. and P.M.; resources, E.S. and D.D.; data curation, S.B. and D.D.; writing—original draft, S.B. and D.D.; preparation, P.M.; writing—review and editing, S.B. and D.D.; visualization, S.B. and D.D.; supervision, E.S.; project administration, E.S. All authors read and agreed to the published version of the manuscript.

Funding: This research received no external funding.

Institutional Review Board Statement: Not applicable.

Informed Consent Statement: Not applicable.

Data Availability Statement: Not applicable.

Acknowledgments: We acknowledge our families for their kind support.

Conflicts of Interest: The authors declare no conflict of interest.

References

1. Zupanc, J.; Vahdat-Pajouh, N.; Schäfer, E. New thermomechanically treated NiTi alloys—A review. *Int. Endod. J.* **2018**, *51*, 1088–1103. [[CrossRef](#)]
2. McGuigan, M.B.; Louca, C.; Duncan, H.F. The impact of fractured endodontic instruments on treatment outcome. *Br. Dent. J.* **2013**, *214*, 285–289. [[CrossRef](#)]
3. Bueno, C.S.P.; Oliveira, D.P.; Pelegrine, R.A.; Fontana, C.E.; Rocha, D.G.P.; Gutmann, J.L.; Bueno, C.E.S. Fracture incidence of WaveOne Gold files: A prospective clinical study. *Int. Endod. J.* **2020**, *53*, 1192–1198. [[CrossRef](#)]
4. Caballero-Flores, H.; Nabeshima, C.K.; Binotto, E.; Machado, M.E.L. Fracture incidence of instruments from a single-file reciprocating system by students in an endodontic graduate program: A cross-sectional retrospective study. *Int. Endod. J.* **2019**, *52*, 13–18. [[CrossRef](#)]
5. Coelho, M.S.; Rios, M.A.; Bueno, C.E.D.S. Separation of Nickel-Titanium Rotary and Reciprocating Instruments: A Mini-Review of Clinical Studies. *Open Dent. J.* **2018**, *12*, 864–872. [[CrossRef](#)]
6. Yared, G.M.; Dagher, F.E.; Machtou, P.; Kulkarni, G.K. Influence of rotational speed, torque and operator proficiency on failure of Greater Taper files. *Int. Endod. J.* **2002**, *35*, 7–12. [[CrossRef](#)]
7. Zelada, G.; Varela, P.; Martín, B.; Bahillo, J.G.; Magán, F.; Ahn, S. The effect of rotational speed and the curvature of root canals on the breakage of rotary endodontic instruments. *J. Endod.* **2002**, *28*, 540–542. [[CrossRef](#)]
8. Martín, B.; Zelada, G.; Varela, P.; Bahillo, J.G.; Magán, F.; Ahn, S.; Rodríguez, C. Factors influencing the fracture of nickel-titanium rotary instruments. *Int. Endod. J.* **2003**, *36*, 262–266. [[CrossRef](#)]
9. Ferreira, F.; Adeodato, C.; Barbosa, I.; Aboud, L.; Scelza, P.; Zaccaro Scelza, M. Movement kinematics and cyclic fatigue of NiTi rotary instruments: A systematic review. *Int. Endod. J.* **2017**, *50*, 143–152. [[CrossRef](#)]
10. Roland, D.D.; Andelin, W.E.; Browning, D.F.; Hsu, G.-H.R.; Torabinejad, M. The effect of preflaring on the rates of separation for 0.04 taper nickel titanium rotary instruments. *J. Endod.* **2002**, *28*, 543–545. [[CrossRef](#)]

11. Patiño, P.V.; Biedma, B.M.; Liébana, C.R.; Cantatore, G.; Bahillo, J.G. The influence of manual glide path on the separation rate of NiTi rotary instruments. *J. Endod.* **2005**, *31*, 114–116. [[CrossRef](#)] [[PubMed](#)]
12. Parashos, P.; Gordon, I.; Messer, H.H. Factors influencing defects of rotary nickel-titanium instruments after clinical use. *J. Endod.* **2004**, *30*, 722–725. [[CrossRef](#)] [[PubMed](#)]
13. Hilfer, P.B.; Bergeron, B.E.; Mayerchak, M.J.; Roberts, H.W.; Jeansonne, B.G. Multiple autoclave cycle effects on cyclic fatigue of nickel-titanium rotary files produced by new manufacturing methods. *J. Endod.* **2011**, *37*, 72–74. [[CrossRef](#)] [[PubMed](#)]
14. Gambarini, G.; Galli, M.; Di Nardo, D.; Seracchiani, M.; Donfrancesco, O.; Testarelli, L. Differences in cyclic fatigue lifespan between two different heat treated NiTi endodontic rotary instruments: WaveOne Gold vs EdgeOne Fire. *J. Clin. Exp. Dent.* **2019**, *11*, 609–613. [[CrossRef](#)] [[PubMed](#)]
15. Haikel, Y.; Serfaty, R.; Bateman, G.; Senger, B.; Allemann, C. Dynamic and cyclic fatigue of engine-driven rotary nickel-titanium endodontic instruments. *J. Endod.* **1999**, *25*, 434–440. [[CrossRef](#)]
16. Grande, N.M.; Plotino, G.; Pecci, R.; Bedini, R.; Malagnino, V.A.; Somma, F. Cyclic fatigue resistance and three-dimensional analysis of instruments from two nickel-titanium rotary systems. *Int. Endod. J.* **2006**, *39*, 755–763. [[CrossRef](#)]
17. Gomes, M.S.; Vieira, R.M.; Böttcher, D.E.; Plotino, G.; Celeste, R.K.; Rossi-Fedele, G. Clinical fracture incidence of rotary and reciprocating NiTi files: A systematic review and meta-regression. *Aust. Endod. J.* **2021**, in press. [[CrossRef](#)]
18. Madarati, A.A. Factors influencing incidents of complications while using nickel-titanium rotary instruments for root canal treatment. *BMC Oral Health* **2019**, *19*, 241. [[CrossRef](#)]
19. Sattapan, B.; Nervo, G.J.; Palamara, J.E.; Messer, H.H. Defects in rotary nickel-titanium files after clinical use. *J. Endod.* **2000**, *26*, 161–165. [[CrossRef](#)]
20. Plotino, G.; Grande, N.M.; Cordaro, M.; Testarelli, L.; Gambarini, G. A review of cyclic fatigue testing of nickel-titanium rotary instruments. *J. Endod.* **2009**, *35*, 1469–1476. [[CrossRef](#)]
21. Setzer, F.C.; Böhme, C.P. Influence of combined cyclic fatigue and torsional stress on the fracture point of nickel-titanium rotary instruments. *J. Endod.* **2013**, *39*, 133–137. [[CrossRef](#)] [[PubMed](#)]
22. Topcuoglu, H.S.; Topcuoglu, G.; Kafdag, Ö.; Arslan, H. Cyclic fatigue resistance of new reciprocating glide path files in 45- and 60-degree curved canals. *Int. Endod. J.* **2018**, *51*, 1053–1058. [[CrossRef](#)]
23. International Organization for Standardization. *International Standard ISO 3630-1:2019(E): Dentistry—Endodontic Instruments—Part 1: General Requirements*, 3rd ed.; International Organization for Standardization: Geneva, Switzerland, 2019.
24. Hülsmann, M.; Donnermeyer, D.; Schäfer, E. A critical appraisal of studies on cyclic fatigue resistance of engine-driven endodontic instruments. *Int. Endod. J.* **2019**, *52*, 1427–1445. [[CrossRef](#)] [[PubMed](#)]
25. Özyürek, T.; Gündoğar, M.; Uslu, G.; Yılmaz, K.; Staffoli, S.; Nm, G.; Plotino, G.; Polimeni, A. Cyclic fatigue resistances of Hyflex EDM, WaveOne gold, Reciproc blue and 2shape NiTi rotary files in different artificial canals. *Odontology* **2018**, *106*, 408–413. [[CrossRef](#)] [[PubMed](#)]
26. Dederich, D.N.; Zakariassen, K.L. The effects of cyclical axial motion on rotary endodontic instrument fatigue. *Oral Surg. Oral Med. Oral Pathol.* **1986**, *61*, 192–196. [[CrossRef](#)]
27. Gündoğar, M.; Özyürek, T.; Yılmaz, K.; Uslu, G. Cyclic fatigue resistance of HyFlex EDM, Reciproc Blue, WaveOne Gold, and Twisted File Adaptive rotary files under different temperatures and ambient conditions. *J. Dent. Res. Dent. Clin. Dent. Prospects* **2019**, *13*, 166–171. [[CrossRef](#)] [[PubMed](#)]
28. Jamleh, A.; Yahata, Y.; Ebihara, A.; Atmeh, A.R.; Bakhsh, T.; Suda, H. Performance of NiTi endodontic instrument under different temperatures. *Odontology* **2016**, *104*, 324–328. [[CrossRef](#)]
29. Dosanjh, A.; Paurazas, S.; Askar, M. The effect of temperature on cyclic fatigue of nickel-titanium rotary endodontic instruments. *J. Endod.* **2017**, *43*, 823–826. [[CrossRef](#)] [[PubMed](#)]
30. de Vasconcelos, R.A.; Murphy, S.; Carvalho, C.A.; Govindjee, R.G.; Govindjee, S.; Peters, O.A. Evidence for reduced fatigue resistance of contemporary rotary instruments exposed to body temperature. *J. Endod.* **2016**, *42*, 782–787. [[CrossRef](#)] [[PubMed](#)]
31. Klymus, M.E.; Alcalde, M.P.; Vivan, R.R.; Só, M.V.R.; de Vasconcelos, B.C.; Duarte, M.A.H. Effect of temperature on the cyclic fatigue resistance of thermally treated reciprocating instruments. *Clin. Oral Investig.* **2019**, *23*, 3047–3052. [[CrossRef](#)] [[PubMed](#)]
32. Plotino, G.; Grande, N.; Mazza, C.; Petrovic, R.; Testarelli, L.; Gambarini, G. Influence of size and taper of artificial canals on the trajectory of NiTi instruments in cyclic fatigue studies. *Oral Surg. Oral Med. Oral Pathol. Oral Radiol. Endod.* **2010**, *109*, 60–66. [[CrossRef](#)] [[PubMed](#)]
33. Lo Savio, F.; La Rosa, G.; Bonfanti, M.; Alizzio, D.; Rapisarda, E.; Pedullà, E. Novel cyclic fatigue testing machine for endodontic files. *Exp. Tech.* **2020**, *44*, 649–665. [[CrossRef](#)]
34. Zubizarreta-Macho, Á.; Albaladejo Martínez, A.; Falcão Costa, C.; Quispe-López, N.; Agustín-Panadero, R.; Mena-Álvarez, J. Influence of the type of reciprocating motion on the cyclic fatigue resistance of reciprocating files in a dynamic model. *BMC Oral Health* **2021**, *21*, 179. [[CrossRef](#)] [[PubMed](#)]
35. Zubizarreta-Macho, Á.; Mena Álvarez, J.; Albaladejo Martínez, A.; Segura-Egea, J.J.; Caviades Brucheli, J.; Agustín-Panadero, R.; López Piriz, R.; Alonso-Ezpeleta, Ó. Influence of the pecking motion frequency on the cyclic fatigue resistance of endodontic rotary files. *J. Clin. Med.* **2020**, *9*, 45. [[CrossRef](#)] [[PubMed](#)]
36. Plotino, G.; Grande, N.M.; Sorci, E.; Malagnino, V.A.; Somma, F. A comparison of cyclic fatigue between used and new Mtwo Ni-Ti rotary instruments. *Int. Endod. J.* **2006**, *39*, 716–723. [[CrossRef](#)]

37. Anderson, T.L.; Anderson, T.L. *Fracture Mechanics: Fundamentals and Applications*, 3rd ed.; CRC Press: Boca Raton, FL, USA, 2005. [[CrossRef](#)]
38. Cheung, G.S.; Darvell, B.W. Fatigue testing of a NiTi rotary instrument. Part 2: Fractographic analysis. *Int. Endod. J.* **2007**, *40*, 619–625. [[CrossRef](#)] [[PubMed](#)]
39. Schneider, S.W. A comparison of canal preparations in straight and curved root canals. *Oral Surg. Oral Med. Oral Pathol.* **1971**, *32*, 271–275. [[CrossRef](#)]
40. Pruett, J.P.; Clement, D.J.; Carnes, D.L., Jr. Cyclic fatigue testing of nickel-titanium endodontic instruments. *J. Endod.* **1997**, *23*, 77–85. [[CrossRef](#)]
41. Schäfer, E.; Diez, C.; Hoppe, W.; Tepel, J. Roentgenographic investigation of frequency and degree of canal curvatures in human permanent teeth. *J. Endod.* **2002**, *28*, 211–216. [[CrossRef](#)]
42. de Hemptinne, F.; Slaus, G.; Vandendael, M.; Jacquet, W.; De Moor, R.J.; Bottenberg, P. In vivo intracanal temperature evolution during endodontic treatment after the injection of room temperature or preheated sodium hypochlorite. *J. Endod.* **2015**, *41*, 1112–1115. [[CrossRef](#)] [[PubMed](#)]
43. Plotino, G.; Grande, N.M.; Cordaro, M.; Testarelli, L.; Gambarini, G. Influence of the shape of artificial canals on the fatigue resistance of NiTi rotary instruments. *Int. Endod. J.* **2010**, *43*, 69–75. [[CrossRef](#)] [[PubMed](#)]
44. Gambarini, G. Fatigue resistance of new and used nickel-titanium rotating instruments: A comparative study. *Clin. Ter.* **2018**, *169*, 96–101. [[CrossRef](#)]
45. Pedullà, E.; Lo Savio, F.; Boninelli, S.; Plotino, G.; Grande, N.M.; Rapisada, E.; La Rosa, G. Influence of cyclic torsional preloading on cyclic fatigue resistance of nickel–titanium instruments. *Int. Endod. J.* **2015**, *48*, 1043–1050. [[CrossRef](#)] [[PubMed](#)]
46. Alapati, S.B.; Brantley, W.A.; Svec, T.A.; Powers, J.M.; Nusstein, J.M.; Daehn, G.S. SEM observations of nickel-titanium rotary endodontic instruments that fractured during clinical use. *J. Endod.* **2005**, *31*, 40–43. [[CrossRef](#)] [[PubMed](#)]